RSC Advances

PAPER

View Article Online
View Journal | View Issue

Cite this: *RSC Adv.*, 2026, **16**, 20747

TAPP-based fluorescent probes for selective cysteine detection: insights into structure–reactivity relationships

Eren Sahin Gocen, Fatma Demirtas, Hande Akar and Guler Yagiz Erdemir *

Herein, a series of TAPP-based π-conjugated fluorescent probes functionalized with aldehyde, malononitrile, and cyanoacrylate groups were designed and synthesized to investigate structure–reactivity relationships in cysteine (Cys) sensing. The photophysical properties of the probes were systematically examined in THF, DCM, and DMSO. The results revealed that the absorption and emission features are primarily governed by π–π* transitions localized on the TAPP framework, while the terminal acceptor groups mainly modulate the electronic distribution without significantly altering the ground-state transitions. Among the investigated derivatives, only the aldehyde-functionalized probe exhibited a pronounced "turn-on" fluorescence response toward Cys. This behavior is attributed to a reaction-based sensing mechanism involving the formation of a thiazolidine ring between the aldehyde group and Cys. The proposed mechanism is supported by complementary spectroscopic analyses, including ^{1}H NMR and HRMS, which confirm the consumption of the aldehyde group and the formation of a new product species. The probe displayed rapid response kinetics, reaching a stable fluorescence signal within approximately 50 s, and exhibited high selectivity for glutathione (GSH) over *N*-acetylcysteine (NAC), other amino acids, inorganic sulfur species, and metal ions. Fluorescence titration experiments showed a linear response over 0–15 μM, with a low limit of detection (LOD) of 0.37 μM. Furthermore, pH-dependent studies demonstrated that the probe operates effectively under near-physiological conditions. Spiking experiments yielded satisfactory recovery values, confirming its practical applicability. Overall, this study not only presents a sensitive and selective fluorescent probe for cysteine detection but also provides mechanistic insight into how terminal group functionality governs reaction-based sensing behavior in TAPP-based systems.

Received 9th March 2026
Accepted 6th April 2026

DOI: 10.1039/d6ra02033j

rsc.li/rsc-advances

Introduction

Cysteine (Cys), homocysteine (Hcy), and glutathione (GSH) are biothiol molecules that play an important role in maintaining redox balance, protein folding, and regulating cellular metabolism in biological systems. In particular, the association of abnormal changes in Cys levels with neurological diseases, liver damage, and certain types of tumors has made the selective and sensitive determination of this molecule important.[1,2] Therefore, efforts to develop fluorescent probes for the rapid and reliable detection of Cys have increased significantly in recent years. A large portion of the biothiol sensors reported in the literature are based on reaction-based mechanisms that exploit the high nucleophilicity of the thiol group. In this context, reactions such as Michael addition, imine or hemithioacetal formation, nucleophilic ring opening, and disulfide exchange are among the frequently used strategies.[3–5] However, the presence of other thiols, such as GSH and NAC, which are abundant in biological environments, makes it difficult to achieve high selectivity for Cys.[6–17]

In this context, π-conjugated D–A or D–π–A systems with strong fluorescence are widely used in the design of thiol sensors. In particular, systems containing thiol-reactive functional groups such as aldehydes, acrylates, and malononitriles can exhibit "turn-on" fluorescence behavior as a result of covalent reactions with Cys.[18] Among such systems, tetraaryl-1,4-dihydropyrrolo[3,2-*b*]pyrrole (TAPP) derivatives and their extended analogs are noteworthy due to their rigid and planar molecular structures, high photostability, and strong fluorescence yields. Furthermore, the ease with which the TAPP core can be functionalized at terminal positions allows for the comparative study of different reactive groups on the same.

In this study, three different TAPP-based fluorescent molecules carrying aldehyde, malononitrile, and cyanoacrylate functional groups were designed and synthesized. The aim was to compare the effects of different terminal groups on Cys detection behavior on the same conjugated fluorophore platform. The photophysical properties were studied in detail in different solvents, and selectivity against biothiol species was

Gazi University, Faculty of Science, Department of Chemistry, 06560, Ankara, Turkiye. E-mail: guleryagiz@gazi.edu.tr

tested. The studies revealed that only the derivative bearing the aldehyde functional group exhibited a distinct "turn-on" fluorescence response towards Cys. The results indicate that not only the electron-withdrawing effect but also the functional group's geometric accessibility and reactivity are decisive for Cys detection.

Experimental

Materials and methods

All reagents and solvents were purchased from commercial sources. The urine used in this study was a commercially available urine reference material (Seronorm™L1) obtained from Sero AS (Billingstad, Norway). The reaction progress was monitored by thin-layer chromatography (TLC), performed on silica gel 60. pH measurements were carried out using a Mettler-Toledo S210 pH meter. The identity of the prepared compounds was confirmed by FTIR, ^{1}H NMR, ^{13}C NMR, and HRMS (QTOF). NMR spectra were measured on a Varian 500 MHz instrument at Gazi University. Chemical shifts (δ, ppm) were determined with tetramethylsilane (TMS) as the internal reference; J values are given in Hz. ^{1}H NMR spectra were recorded in $CDCl_3$ (δ_H 7.26 ppm as residual solvent peak) and ^{13}C NMR spectra in $CDCl_3$ (δ_C 77.16 ppm). UV-vis spectra were measured using a T80+ double beam UV-vis spectrophotometer from PG Instruments Ltd Emission spectra were measured using a Hitachi F-7000 fluorescence spectrophotometer, and fluorescence measurements were carried out with a slit width of 5 nm and a PMT voltage of 950 V. All spectroscopic measurements were carried out at a concentration of 10^{-6} M to avoid aggregation and inner-filter effects.

Synthesis of 2,5-bis(4-bromophenyl)-1,4-di-*p*-tolyl-1,4-dihydropyrrolo[3,2-*b*]pyrrole (3) ($C_{32}H_{24}Br_2N_2$). Glacial acetic acid (2 mL), toluene (2 mL), *p*-bromobenzaldehyde (4 mmol), and *p*-methylaniline (4 mmol) were placed in a 50 mL round-bottom flask equipped with a magnetic stir bar. The mixture was heated at 50 °C for 1 h. After that time, $Fe(ClO_4)_3xH_2O$ (6 mol%) was added, followed by butane-2,3-dione (2 mmol). The resulting mixture was stirred at 50 °C (in an oil bath) in an open flask overnight. The oil bath was removed, and 5 mL of methanol was added to the reaction mixture. The resulting precipitate was filtered off, washed with methanol (10 mL), and dried under vacuum to afford pure product **3** as a cream solid.[19]

Synthesis of 4-(5-(4-bromophenyl)-1,4-di-*p*-tolyl-1,4-dihydropyrrolo[3,2-*b*]pyrrol-2-yl)benzonitrile (4) ($C_{33}H_{24}BrN_3$). Compound **3** (1 mmol) and CuCN (1.2 mmol) were dissolved in 25 mL of *N*-methylpyrrolidone (NMP) solvent. The resulting mixture was heated under an argon atmosphere at 150 °C for 72 hours. After the reaction was complete, the solvent was removed under vacuum. The resulting residue was washed three times with dichloromethane (20 mL), then dried over anhydrous sodium sulphate, and the solvent was removed again. The crude product was purified by filtration using silica gel with a 1 : 1 (v/v) DCM/hexane eluent. Fractions with an R_f value of 0.25 were collected, and the target derivative **4** was obtained by removing the solvent.[20]

Synthesis of 4-(5-(4′-formyl-[1,1′-biphenyl]-4-yl)-1,4-di-*p*-tolyl-1,4-dihydropyrrolo[3,2-*b*]pyrrol-2-yl)benzonitrile (5) ($C_{40}H_{29}ON_3$). In an inert atmosphere, 4-(5-(4-bromophenyl)-1,4-di-*p*-tolyl-1,4-dihydropyrrolo[3,2-*b*]pyrrol-2-yl)benzonitrile (**4**) (0.5 mmol) was dissolved in 10 : 5 mL of THF : H_2O. After that, potassium carbonate (6 mmol) and (4-formylphenyl)boronic acid (1.2 mmol) were added to this solution, respectively. The reaction mixture was stirred for 10 min, the palladium catalyst was added, and the mixture was heated under a reflux condenser for 24 h. After the reaction was complete, it was cooled, then poured into ice–cold water (50 mL), and the mixture was extracted twice with DCM (25 mL). The organic phases were collected, and the solvent was removed. The obtained derivative **5** was purified by column chromatography on silica gel using a DCM/hexane (6/4) solvent system.[21]

Synthesis of 2-((4′-(5-(4-cyanophenyl)-1,4-di-*p*-tolyl-1,4-dihydropyrrolo[3,2-*b*]pyrrol-2-yl)-[1,1′-biphenyl]-4-yl)methylene) malononitrile (6) ($C_{49}H_{33}N_5$). In a 10 mL flask under an argon atmosphere, Et_3N (0.1 mL) was added to a solution of malononitrile (2 mmol) and the derivative of **5** (1 mmol) in $CHCl_3$. The reaction mixture was stirred overnight at 80 °C and treated with brine after the starting material had been consumed (monitored by TLC). The organic phase was dried over Na_2SO_4, and the crude product was purified by chromatography column [silica gel, DCM : hexane (7 : 3)] and recrystallization from methanol.

Synthesis of ethyl 2-cyano-3-(4′-(5-(4-cyanophenyl)-1,4-di-*p*-tolyl-1,4-dihydropyrrolo[3,2-*b*]pyrrol-2-yl)-[1,1′-biphenyl]-4-yl) acrylate (7) ($C_{45}H_{35}O_2N_4$). In a 10 mL flask under an argon atmosphere, Et_3N (0.1 mL) was added to a solution of ethyl cyanoacetate (2 mmol) and derivative **5** (1 mmol) in $CHCl_3$. The reaction mixture was stirred overnight at 80 °C and treated with brine after the starting material had been consumed (monitored by TLC). The organic phase was dried over Na_2SO_4, and the crude product was purified by chromatography column [silica gel, DCM : hexane (7 : 3)] and recrystallization from methanol.

General procedure for spectral measurements. The stock solutions of the probe compounds were prepared in 10^{-6} M DMSO and further diluted to 10^{-7} M for experimental measurements. Measurement solutions were prepared by mixing 1% (v/v) probe solution with 99% (v/v) phosphate-buffered saline (PBS, 0.1 M, pH 7.4). Stock solutions of analytes (Cys, GSH, Hcy, Ala, Met, Thr, Lys, NAC, Na_2S, NaHS, $CaCl_2$, $MgCl_2$, $FeCl_2$) were prepared in double-distilled water and diluted to the desired concentrations with PBS as needed. All analyte standards were of high purity (>99%) and commercially available; relevant stereochemical characteristics and sources are provided in the SI. For typical UV-vis absorption and fluorescence measurements, 2.0 mL of the prepared probe solution was placed in a 1 cm quartz cuvette, and spectral measurements were performed after the addition of the analytes in the specified volumes. UV-vis absorption and fluorescence emission spectra were recorded at room temperature.

Results and discussion

Molecular structure: design, synthesis, and characterization

In this study, three different TAPP-based π-conjugated molecules were designed and synthesized to develop fluorescent sensor candidates for the selective detection of thiol-containing biomolecules (Scheme 1). In this study, various terminal groups attached to the TAPP core were selected not only based on their potential for covalent reactions with cysteine but also with the aim of modulating the core's electronic structure and intramolecular charge transfer (ICT) characteristics. The electron distribution and polarity of the molecule were controlled by introducing aromatic and electron-withdrawing groups at the 2,5-positions, thereby enabling a comparative analysis of the electronic effects of different terminal groups. This approach facilitates a better understanding of the structural and electronic foundations of fluorescence properties and selectivity. The aldehyde-containing derivative (**5**) possesses a reactive center capable of forming a covalent bond with cysteine and has exhibited distinct reaction-based sensing behavior. In contrast, malononitrile and cyanoacrylate derivatives cannot form direct covalent bonds; however, their strong electron-withdrawing properties modulate the fluorescence behavior by influencing the ICT character. These derivatives have been used not as direct reactive sensors but as comparative systems, revealing the role of terminal group electronic effects on structural and photophysical outcomes. Thanks to this approach, the differences between the contributions of various terminal groups and their reaction-based behaviors have been analyzed both quantitatively and qualitatively in terms of electronic structure and ICT character, and the structural basis for the observed selectivity and fluorescence changes has been more clearly elucidated.[22–28]

The structural characterization of the obtained compounds was performed using FTIR, ^{1}H, and ^{13}C NMR spectroscopy; their molecular masses were confirmed by high-resolution mass spectrometry (HRMS). In the FTIR spectra, characteristic C–H stretching vibrations associated with aromatic rings were observed in the 3030–3060 cm^{-1} region for all compounds. C=C and C=N stretching bands representing the conjugated structure of the TAPP core were clearly detected in the 1580–1620 cm^{-1} range. In the aldehyde-containing derivative, the carbonyl stretching band was observed around 1695 cm^{-1}, while weak C–H bands corresponding to the formyl group appeared in the 2710–2840 cm^{-1} range. In the acrylate derivative, a strong band corresponding to the ester carbonyl was observed at approximately 1726 cm^{-1}. In derivatives containing a nitrile group, a sharp band corresponding to the –CN stretching was clearly observed in the 2210–2220 cm^{-1} region. Particularly in the malononitrile derivative, the higher intensity of this band is consistent with the presence of two nitrile groups in the structure (Fig. SI 1, 3, 7, 10).

Following this structural characterization, the photophysical properties of the compounds were investigated. UV-vis absorption measurements revealed distinct solvochromic shifts in the π–π* and ICT transition bands, depending on the solvent polarity. This indicates that the molecules possess an electronic structure sensitive to changes in environmental polarity. Fluorescence measurements revealed that the compounds exhibited different emission profiles in different solvents (THF, DCM, and DMSO). These results indicate that TAPP-based conjugated systems exhibit ICT character and have the potential to generate

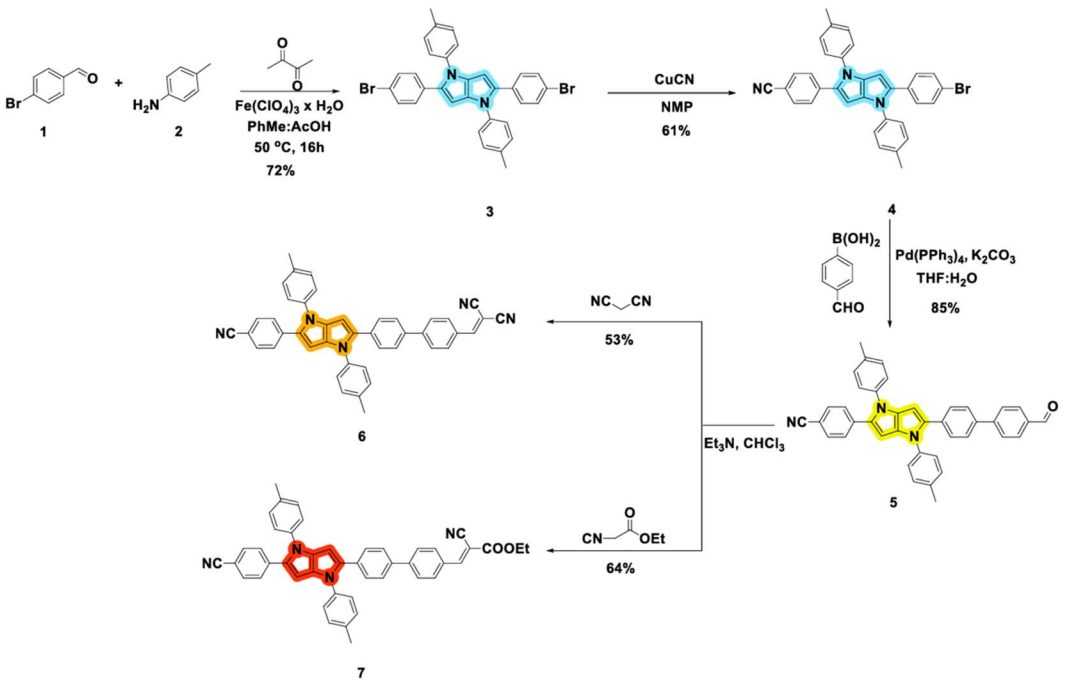

Scheme 1 The synthesis pathway.

measurable fluorescence changes through chemical interactions with thiol species (Fig. SI 13–17).[29,30]

Photophysical properties

Photophysical behavior in solvent media

The UV-vis absorption and fluorescence emission properties of compounds **5–7** were studied in detail at a concentration of 10^{-6} M in THF, DCM, and DMSO solvents (Table 1 and Fig. SI 15–17). All compounds exhibited characteristic absorption bands in the visible region, which are primarily attributed to π–π* transitions centered on the TAPP core. The absorption maxima of the three derivatives lie within a very narrow spectral range, indicating that, despite the presence of different electron-withdrawing terminal groups, the electronic transitions are largely localized on the conjugated TAPP skeleton. This suggests that a dominant intramolecular charge transfer (ICT) character does not prevail throughout the molecule.

This behavior can be explained by the partially limited electronic communication between the TAPP core and the terminal acceptor groups. One contributing factor is the inherent non-planarity of the biphenyl bridge, which arises from steric hindrance between the ortho hydrogens. This steric effect restricts conjugation even in the absence of rotation, and the additional conformational flexibility of the biphenyl further reduces planarity. Similar effects have been reported in D–π–A systems containing rotatable aromatic linkers, where deviations from planarity reduce HOMO–LUMO overlap and consequently prevent significant bathochromic shifts in the absorption spectra.[31,32] Literature studies specifically on biphenyl derivatives also highlight this intrinsic non-planarity due to steric interactions.[33]

Examination of the fluorescence emission spectra revealed relatively small changes in the emission maxima but noticeable differences in fluorescence quantum yields with solvent polarity (Fig. SI 19). In general, higher fluorescence intensities were obtained in the THF medium, whereas a decrease in emission intensity was observed in some derivatives in the more polar solvents DCM and DMSO. This behavior can be attributed to increased solvent-molecule interactions and vibrational relaxation processes in polar solvents, which enhance non-radiative decay pathways in the excited state.[34–36] Among the investigated derivatives, compounds **6** and **7**, which contain strong electron-withdrawing groups, did not exhibit a significant bathochromic shift compared to compound **5**, bearing a formyl group. This observation indicates that the photophysical properties are not determined solely by the electronic nature of the terminal substituents. Instead, steric and conformational factors may also play an important role. The relatively small size of the formyl group may allow a more favorable geometric alignment with the aromatic ring, enabling more efficient electronic interaction with the TAPP core. Overall, the photophysical data indicate that the TAPP core acts as the dominant chromophoric unit in this molecular design, while the terminal functional groups exert a limited influence on the ground-state absorption properties. This feature is particularly important for sensing studies, as it suggests that the observed fluorescence changes may arise primarily from reaction-induced structural changes upon analyte interaction rather than from a strong ground-state ICT effect, thereby providing a suitable platform for selective fluorescence sensing (Fig. 1).

Cysteine sensitivity and selectivity studies

To evaluate the potential chemical sensor properties of compound **5**, the fluorescence behavior in the presence of Cys in solution was systematically investigated. Initial screening experiments were conducted at a concentration of 10^{-7} M, and only compound **5** showed a significant increase in fluorescence upon addition of Cys. In contrast, no significant emission change was observed in derivatives modified with terminal acceptor groups malononitrile (**6**) and cyanoacrylate (**7**) in the presence of Cys. This indicates that the aldehyde function plays a decisive role in the formation of the fluorescence response based on interaction with Cys. To evaluate the selectivity of the observed fluorescence response, the fluorescence behavior of compound **5** was studied in detail in the presence of different biological and chemical species. In this context, homocysteine (Hcy), glutathione (GSH), histidine (His), lysine (Lys), methionine (Met), threonine (Thr), *N*-acetylcysteine (NAC), alanine (Ala), Na_2S, NaHS, $CaCl_2$, $MgCl_2$, and $FeCl_2$ were added to the system separately, and the fluorescence spectra were recorded. The results obtained show that none of the species studied

Table 1 Photophysical properties of derivatives 5–7 obtained in THF, DCM and DMSO (10^{-6} M)[a]

Comp.	Solvent	$\lambda_{max\ (Ab)}$ (nm)	$\varepsilon@\lambda_{max}$ ($M^{-1}\ cm^{-1}$)	$\lambda_{max(Em)}$ (nm)	Stokes shift (cm^{-1})	Φ_{fl}
5	THF	412	16180	528	5330	0.59
	DCM	419	35750	528	4920	0.26
	DMSO	412	10300	486	3690	0.33
6	THF	412	16060	480	3430	0.58
	DCM	412	13600	480	3440	0.14
	DMSO	412	26020	482	3520	0.60
7	THF	423	20800	471	2410	0.23
	DCM	435	57630	478	2070	0.04
	DMSO	430	31690	455	1270	0.37

[a] Standard: cumarine 153 in EtOH ($\Phi_{fl} = 0.54$).

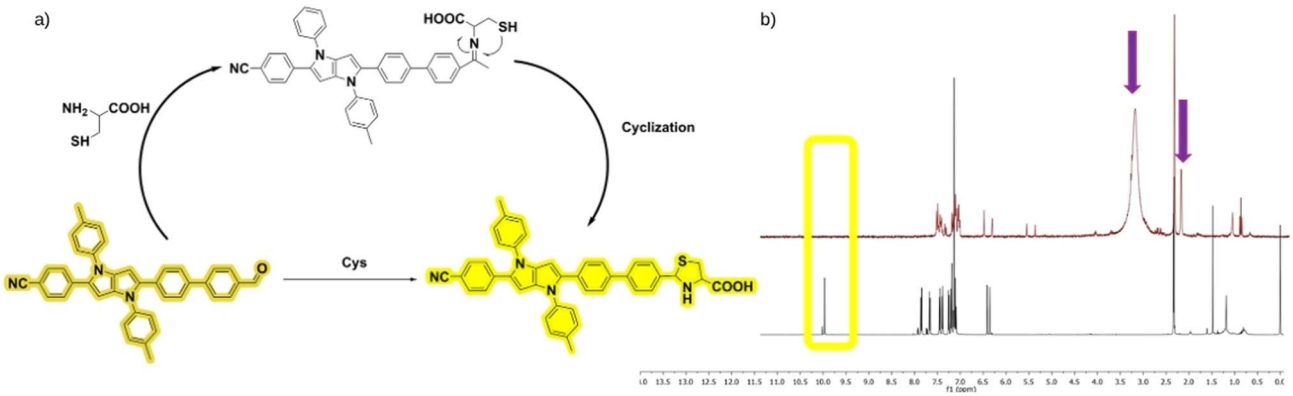

Fig. 1 (a) The response mechanism of **5** to Cys (b) partial ^{1}H NMR spectra of **5** (2 mg) upon the addition of Cys (2 eqv.) in $CDCl_3$ at 25 °C: (i) without Cys (ii) after adding Cys.[29,30]

produced a fluorescence increase comparable to that of Cys (Fig. 2).

The fact that GSH and NAC, thiol-containing species found in high concentrations, especially in biological environments, do not produce a significant fluorescence response indicates that compound **5** exhibits high selectivity for Cys. Furthermore, the lack of a noticeable increase in fluorescence for Hcy, which differs from Cys by only a methylene group, demonstrates that the developed probe can distinguish between Cys and Hcy. This result indicates that selectivity depends not only on thiol reactivity but also on geometric factors related to ring formation. The observed selective fluorescence behaviour is consistent with the detection mechanism based on the aldehyde-Cys reaction, which has been widely reported in the literature. As is known, aldehyde groups can react with the $-NH_2$ and $-SH$ functional groups of Cys to form a five-membered thiazolidine ring. The structural transformation resulting from this reaction can alter the system's electronic properties, leading to a "turn-on" increase in fluorescence. In contrast, the absence of both functional groups in other amino acids, or the presence of steric hindrance in larger biomolecules such as GSH, prevents a similar reaction from occurring, thereby limiting the formation of a fluorescence response. In this study, only compound **5** shows a fluorescence response in the presence of Cys, consistent with this mechanism. In contrast, modifying the formyl group in compounds **6** and **7** with malononitrile and cyanoacrylate derivatives prevents the occurrence of a fluorescence response by inhibiting a similar covalent interaction with Cys. Furthermore, the lack of response from GSH and NAC, which are larger thiol-containing species, indicates that steric effects and functional group arrangement play an important role in selectivity. Taken together, these results indicate that the selective "turn-on" fluorescence response observed for compound **5** toward Cys stems from a reaction-based sensing mechanism rather than random thiol interactions (Fig. 1).

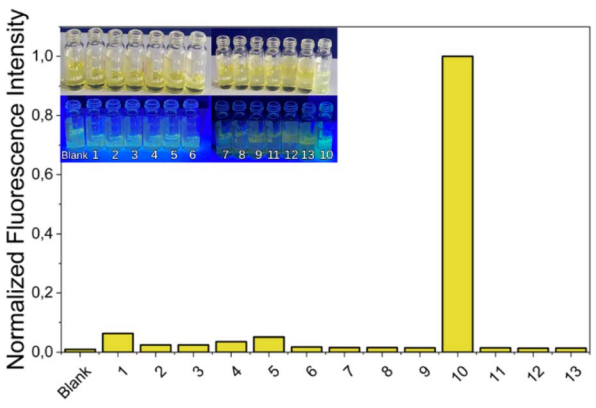

Fig. 2 Normalized fluorescence intensity changes of probe 5 (0.1 μM) upon the addition of various analytes [1: GSH, 2: Hist, 3: Lys, 4: Met, 5: Hcy, 6: Ala, 7: Na_2S, 8: Thr, 9: NAC, 10: CYS, 11: $ZnCl_2$, 12: $FeCl_2$, 13: NaHS] (50 μM each) in PBS buffer (pH 7.4).

Effect of pH on the fluorescence response of 5 toward Cys

To evaluate the pH-dependent behaviour of the developed probe, the fluorescence properties of compound **5** were systematically investigated in the pH range of 3–10, both alone and in the presence of Cys. In the system where the probe was present alone, the fluorescence intensity showed a limited increase over the pH range 3–7 and exhibited a relatively stable trend, with a slight decrease above pH 7. This indicates that the TAPP skeleton exhibits relatively stable fluorescence properties over a wide pH range and that the probe alone does not produce a strong pH-sensitive signal. In contrast, a significant increase in probe fluorescence intensity was observed in the presence of Cys. In particular, the fluorescence signal increased markedly over the pH range 5–7. The maintenance of high fluorescence levels at neutral and slightly basic pH values indicates that the detection mechanism can function effectively under physiological pH conditions. The increase in signal observed in the pH range of 8–10 can be attributed to the faster reaction between the aldehyde group and Cys in a basic environment (Fig. 3). Furthermore, the difference between the limited pH dependence observed with the probe alone and the marked increase in fluorescence in the presence of Cys clearly demonstrates that the signal change is due to a selective chemical interaction with

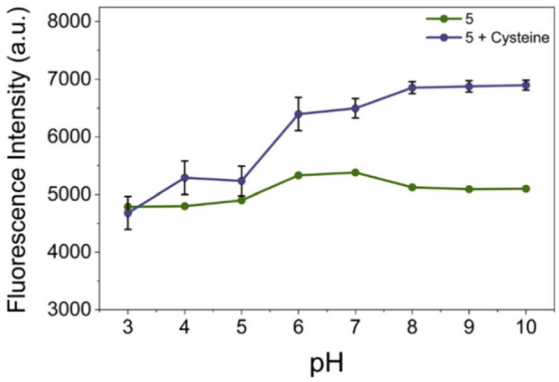

Fig. 3 pH-dependent fluorescence intensity changes of **5** (green line) and **5** in the presence of Cys (blue line) over the pH range 3–10. The probe alone exhibits only minor fluorescence variations, indicating weak intrinsic pH sensitivity. In contrast, a pronounced fluorescence enhancement is observed for **5** upon addition of Cys, particularly in the pH range 5–7, demonstrating that the fluorescence response originates from a specific chemical interaction with Cys rather than from pH effects. Error bars represent the standard deviation of three independent measurements. (Cys: 10^{-2} M).

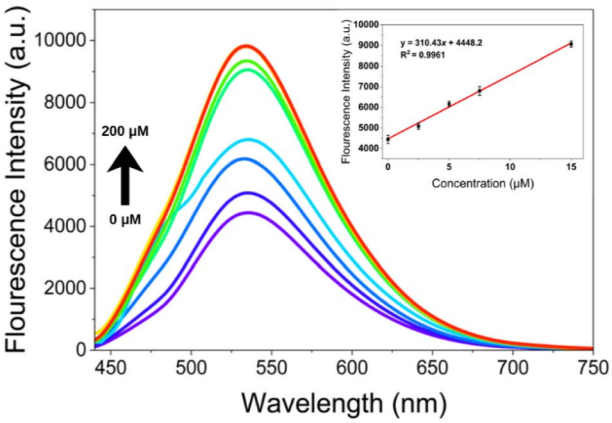

Fig. 4 Fluorescence emission spectra of compound **5** (0.1 μM) upon gradual addition of Cys (0–50 μM) in PBS buffer (pH 7.4). A concentration-dependent fluorescence enhancement is observed. Inset: linear calibration plot of fluorescence intensity *versus* Cys concentration in the range of 0–15 μM ($R^2 = 0.9961$).

Cys rather than pH. These results demonstrate that the developed probe operates stably over a wide pH range and reliably detects Cys at neutral pH, a condition critical for biological systems.

The analytical performance of the probe

Fluorescence titration experiments were conducted to quantitatively evaluate the Cys detection performance of compound **5**. Within this scope, Cys was added to the system at increasing concentrations (0–50 μM), and the corresponding fluorescence emission spectra were recorded after each addition. The measurements showed that the fluorescence signal reached a stable value within approximately 50 s after the addition of Cys. This result demonstrates that the developed probe provides a rapid detection response to Cys. During the experiments, it was observed that the fluorescence emission intensity, which was initially around 3000 a.u., increased steadily with increasing Cys concentration. It was determined that the emission intensity reached approximately 10 000 a.u. at the highest Cys concentration, thus demonstrating that compound **5** exhibits a distinct "turn-on" fluorescence response in the presence of Cys (Fig. 4). This regular increase in the fluorescence signal indicates that a concentration-dependent interaction occurs between compound **5** and Cys. When examining the relationship between Cys concentration and fluorescence intensity, a strong linear relationship was observed over the 0–15 μM range. The calibration curve was expressed by the equation $y = 310.43x + 4448.2$, and the correlation coefficient R^2 was 0.9961. This result shows that compound **5** provides a suitable linear response for quantitative Cys determination over the low-concentration range (Fig. 4, inner graph).

The limit of detection (LOD) and limit of quantification (LOQ) values were calculated to evaluate the analytical performance of the probe. These calculations were performed using the equations $\mathrm{LOD} = 3.3\sigma/m$ and $\mathrm{LOQ} = 10\sigma/m$. Here, σ represents the standard deviation of ten independent blank measurements ($\sigma = 34.57$), and m represents the slope of the calibration curve. The calculations yielded LOD and LOQ values of 0.37 μM and 1.11 μM, respectively. These results demonstrate that compound **5** exhibits high sensitivity toward Cys and can be used reliably as a fluorescence-based detection system, particularly at low micromolar concentrations.

Real sample simulation using spiked samples

Spiking experiments were performed to evaluate the applicability of the developed fluorescent probe (compound **5**) in more complex environments. For this purpose, Cys was added to a PBS buffer solution at a known concentration and analyzed using analytical performance recovery experiments. Quantitative determination was performed using an external calibration curve prepared in buffer medium. The Cys concentration in the spiked samples was calculated from the calibration equation obtained in the buffer solution. The experiments were performed with three parallel measurements, and the results are presented in Table 2. Analysis of the obtained results shows that the average recovery value is 96.5%. These results demonstrate that the analytical response of the developed fluorescent probe can be maintained in spiked samples and provides satisfactory accuracy for Cys determination.

A review of turn-on fluorescent probes for cysteine detection in the literature reveals that systems with diverse structures and mechanisms exhibit high sensitivity and selectivity (Table S1). NIR probes, BODIPY derivatives, and target-specific systems stand out for their low detection limits and suitable response times. However, a significant portion of these systems requires complex synthesis processes or provides limited mechanistic insight. The TAPP-based π-conjugated aldehyde system developed in this study demonstrates competitive performance compared to similar studies in the literature, with both a fast response time (<50 s) and a low detection limit (0.37 μM). In

Table 2 Recovery study for cysteine determination in spiked urine samples

Sample	Added (μM)	Found (μM)	Recovery (%)	RSD (%), $n = 3$
Urine	5.00	4.83	96.5	0.54

particular, the rapid response time on the order of seconds achieved in this study provides a significant advantage compared to response times on the order of minutes in some literature examples. In addition, the proposed system stands out in the literature not only for its analytical performance but also for its design, which enables investigation of the structure–reactivity relationship. The systematic comparison of different terminal groups on the same π-conjugated backbone more clearly reveals the role of electronic effects and functional group reactivity on fluorescence behavior. In particular, the observation of the aldehyde functional group reacting with cysteine to form a thiazolidine ring and the resulting fluorescent "turn-on" response provide a mechanism consistent with the literature and supported by both experimental and theoretical data in this study.

In this regard, the developed probe system not only offers competitive analytical performance but also provides a more comprehensive understanding of the cysteine detection mechanism.[37–41]

Computational studies

Density Functional Theory (DFT) calculations were performed to better understand the electronic structure and sensing mechanism of compound **5**. All calculations were carried out using the ORCA 6.1 software package at the B3LYP functional and 6-31G(d) basis set levels.[42,43] In the frequency analysis performed after optimization, no imaginary frequencies were observed, confirming that the obtained structure corresponds to a true minimum on the potential energy surface. Analysis of the boundary molecular orbitals (HOMO–LUMO) provides important insights into the reactivity of **5**. It was observed that the HOMO orbital is predominantly localized on the TAPP core, whereas the LUMO orbital is distinctly concentrated on the formyl (CHO) group. This spatial separation is consistent with the nature of charge transfer within the molecule and indicates that the aldehyde group acts as an electron-accepting and reactive center. The HOMO and LUMO energy levels were calculated to be −4.9358 eV and −1.8776 eV, respectively, with an energy gap (ΔE) of 3.0581 eV. This value is quite close to the experimentally observed maximum absorption wavelength (412 nm, 3.0093 eV), supporting the reliability of the theoretical method used (Fig. 5).

A molecular electrostatic potential (MEP) map was analyzed to investigate the site selectivity of the nucleophilic attack (Fig. SI 23). The results indicate the presence of a distinct positive potential on the carbonyl carbon of the aldehyde group. This indicates that the carbon atom in question possesses a strong electrophilic character and serves as the most suitable center for the nucleophilic attack by the thiol group of cysteine. In other regions of the molecule, a more neutral or negative potential distribution was observed, suggesting that these regions exhibit lower reactivity toward nucleophiles. When these findings are considered together, it is evident that the selective reaction of **5** with cysteine stems from the electrophilic nature of the aldehyde group and is consistent with the proposed mechanism of thiazolidine formation. Furthermore, these results help explain the reactivity differences among derivatives with different terminal groups, which are determined by their electronic structures.

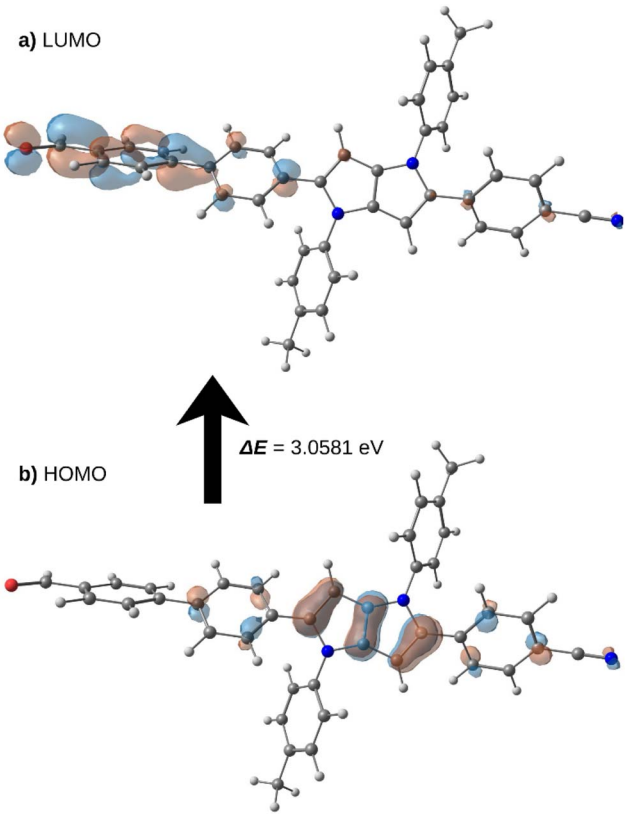

Fig. 5 Optimized geometry and frontier molecular orbitals (a) LUMO and (b) HOMO of compound **5** with the calculated energy gap (ΔE = 3.0581 eV) at the B3LYP/6-31G(d) level.

Conclusion

In this study, three new π-conjugated fluorescent compounds based on the TAPP core and functionalized with aldehyde, malononitrile, and cyanoacrylate groups were successfully synthesized, and their photophysical and sensing properties were systematically investigated. The UV-vis absorption and fluorescence emission behaviors of the compounds were examined in solvents of different polarity. The results indicated that the main optical transitions were predominantly localized on the TAPP framework, while the terminal acceptor groups did not induce a significant bathochromic shift. These observations suggest that molecular planarity and conformational effects play an important role in determining the photophysical

characteristics of these systems. Among the investigated derivatives, the aldehyde-containing compound exhibited a clear "turn-on" fluorescence response toward cysteine (Cys), whereas the malononitrile and cyanoacrylate analogs showed negligible response under the same conditions. Selectivity experiments further demonstrated that the aldehyde-based probe exhibits distinct fluorescence enhancement in the presence of Cys, while remaining largely unresponsive to glutathione (GSH), *N*-acetylcysteine (NAC), other amino acids, inorganic sulfur species, and various metal ions. These results indicate that the probe possesses good selectivity for Cys. In addition, the gradual fluorescence enhancement observed during Cys titration experiments, together with satisfactory recovery values obtained from spiking experiments, indicates that the proposed probe can provide reliable analytical responses under the studied conditions. Overall, the results demonstrate that TAPP-based π-conjugated systems can serve as a useful platform for the development of reaction-based fluorescent probes for cysteine detection. These findings may inform future studies on the design of new selective fluorescent sensing systems.

Author contributions

E. S. G. and F. D.: synthesis, formal analysis, investigation. H. A.: investigation and writing review. G. Y. E.: supervision, conceptualization, project administration, writing, review, and editing. All authors have given approval to the final version of the manuscript.

Conflicts of interest

There are no conflicts to declare.

Data availability

The data supporting this article have been included as part of the supplementary information (SI). Supplementary information is available. See DOI: https://doi.org/10.1039/d6ra02033j.

Acknowledgements

This work is dedicated to Gazi University, named after Gazi Mustafa Kemal Atatürk, the founder of the Republic of Türkiye, in celebration of its 100th anniversary. The authors gratefully acknowledge Prof. Dr Mehmet Sayım Karacan and Prof. Dr Aliye Altundaş for valuable support and contributions throughout this study.

References

1 C. Li, L. Junbo and C. Dugang, *Chin. J. Org. Chem.*, 2021, **41**, 611–623.
2 J. H. Xie, M. Y. Han, L. Meng, N. B. Li, P. Xue and H. Q. Luo, *Sens. Actuators, B*, 2026, **448**, 138986.
3 Y. Liu, D. Yu, S. Ding, Q. Xiao, J. Guo and G. Feng, *ACS Appl. Mater. Interfaces*, 2014, **6**, 17543–17550.
4 L.-Y. Niu, Y.-Z. Chen, H.-R. Zheng, L.-Z. Wu, C.-H. Tung and Q.-Z. Yang, *Chem. Soc. Rev.*, 2015, **44**, 6143–6160.
5 X. Chen, H. Xu, S. Ma, H. Tong, K. Lou and W. Wang, *RSC Adv.*, 2018, **8**, 13388–13392.
6 G. S. Yeom, I.-h. Song, S. D. Warkad, P. B. Shinde, T. Kim, S.-m. Park and S. B. Nimse, *Biosensors*, 2021, **11**, 420.
7 G. Kalaiyarasan, C. Hemlata and J. Joseph, *ACS Omega*, 2019, **4**, 1007–1014.
8 R.-F. Zeng, J.-S. Lan, X.-D. Li, H.-F. Liang, Y. Liao, Y.-J. Lu, T. Zhang and Y. Ding, *Molecules*, 2017, **22**, 1618.
9 J. Lv, X. Jiao, D. D. He, E. Hussain, N. Yang, Y. Wang, H. Zhang, L. Chen, X. Jin and N. Liu, *Anal. Bioanal. Chem.*, 2023, **415**, 4875–4883.
10 C. Y. Ang, S. Y. Tan, Y. Lu, L. Bai, M. Li, P. Li, Q. Zhang, S. T. Selvan and Y. Zhao, *Sci. Rep.*, 2014, **4**, 7057.
11 L. Wu, A. C. Sedgwick, X. Sun, S. D. Bull, X.-P. He and T. D. James, *Acc. Chem. Res.*, 2019, **52**, 2582–2597.
12 J. Kolińska and A. Grzelakowska, *Spectrochim. Acta, Part A*, 2021, **262**, 120151.
13 Z. Huang, C. Wu, Y. Li, Z. Zhou, R. Xie, X. Pang, H. Xu, H. Li and Y. Zhang, *Anal. Methods*, 2019, **11**, 3280–3285.
14 X. Wen, X. Chang, A. Li, X. Yang, F. Tian, Z. Liu, N. Copner, P. Teng and L. Yuan, *Biosens. Bioelectron.*, 2023, **223**, 115021.
15 X. Zeng, X. Zhang, B. Zhu, H. Jia and Y. Li, *Dyes Pigm.*, 2012, **94**, 10–15.
16 X. Rong, C. Liu, Y. Wang, X. Zhao, Z. Wang and B. Zhu, *Sens. Actuators, B*, 2025, **428**, 137232.
17 J. Yang, C. Qian, H. Su, J. Zhang, S. Yu, X. Yu and L. Pu, *Org. Lett.*, 2025, **27**, 571–576.
18 X. Chen, X. Huang, G. Liu, Y. Tu, C. Fan and S. Pu, *Dyes Pigm.*, 2021, **196**, 109810.
19 R. Domínguez, N. F. Montcada, P. de la Cruz, E. Palomares and F. Langa, *ChemPlusChem*, 2017, **82**, 1096–1104.
20 K. Górski, S. Shelton, J. Lingagouder, P. Data, D. Jacquemin and D. T. Gryko, *Chem. Sci.*, 2025, **16**, 5223–5233.
21 O. Cansever and G. Yagiz Erdemir, *ACS Omega*, 2025, **10**, 45671–45679.
22 G. Y. Erdemir, I. Knysh, K. Skonieczny, D. Jacquemin and D. T. Gryko, *J. Org. Chem.*, 2024, **89**, 15513–15522.
23 A. Janiga, D. Bednarska, B. Thorsted, J. Brewer and D. T. Gryko, *Org. Biomol. Chem.*, 2014, **12**, 2874–2881.
24 Ł. G. Łukasiewicz, H. G. Ryu, A. Mikhaylov, C. Azarias, M. Banasiewicz, B. Kozankiewicz, K. H. Ahn, D. Jacquemin, A. Rebane and D. T. Gryko, *Chem. –Asian J.*, 2017, **12**, 1736–1748.
25 S. P. Hashemian, S. M. A. Zanjani, Y. Latifi, M. Behraveshfar and M. B. Teimouri, *Asian J. Org. Chem.*, 2025, **14**, e00565.
26 J. Wang, Z. Chai, S. Liu, M. Fang, K. Chang, M. Han, L. Hong, H. Han, Q. Li and Z. Li, *Chem.–Eur. J.*, 2018, **24**, 18032–18042.
27 M. Krzeszewski, D. Gryko and D. T. Gryko, *Acc. Chem. Res.*, 2017, **50**, 2334–2345.
28 M. Krzeszewski and D. T. Gryko, *J. Org. Chem.*, 2015, **80**, 2893–2899.
29 S. Wang, Y. Huang and X. Guan, *Molecules*, 2021, **26**, 3575.
30 R. Asghar, Y. Li, F. Huo and C. Yin, *Chem. Biomed. Imaging*, 2024, **2**, 250–269.

31 Z. R. Grabowski, K. Rotkiewicz and W. Rettig, *Chem. Rev.*, 2003, **103**, 3899–4032.
32 W. Rettig, *Angew Chem. Int. Ed. Engl.*, 1986, **25**, 971–988.
33 B. Landeros-Rivera and J. Hernández-Trujillo, *ChemPlusChem*, 2022, **87**, e202100492.
34 J. R. Lakowicz, *Principles of Fluorescence Spectroscopy*, Springer, 2006.
35 W. Li, Y. Pan, L. Yao, H. Liu, S. Zhang, C. Wang, F. Shen, P. Lu, B. Yang and Y. Ma, *Adv. Opt. Mater.*, 2014, **2**, 892.
36 L. Yao, S. Zhang, R. Wang, W. Li, F. Shen, B. Yang and Y. Ma, *Angew. Chem.*, 2014, **126**, 2151.
37 Y. Hu, L. Lu, S. Guo, X. Wu, J. Zhang, C. Zhou, H. Fu and Y. She, *Sens. Actuators, B*, 2023, **382**, 133534.
38 X. Yang, J. Wang, Z. Zhang, B. Zhang, X. Du, J. Zhang and J. Wang, *Food Chem.*, 2023, **416**, 135730.
39 Z. Yang, X. Kang, J. Li, L. Li, X. Ye, X. Liu, K. Chen, Y. Deng, C. Peng and B. Ren, *Food Chem.*, 2024, **456**, 140064.
40 S. An, Y. Lin, T. Ye, T. Bai, D. He, L. Guo, Z. Qian, L. Li, H. Liu and J. Wang, *Talanta*, 2024, **267**, 125247.
41 P. M. Sonawane, N. Jain, J. Kim, S. Jeong Park, S. V. Mulay, S. Balasaheb Nimse and D. G. Churchill, *Chem.–Eur. J.*, 2025, **31**, e202402840.
42 F. Neese, *Wiley Interdiscip. Rev.: Comput. Mol. Sci.*, 2025, **15**, e70019.
43 F. Neese, *J. Comput. Chem.*, 2023, **44**, 381–396.